Quantifying quantum entanglement via a hybrid quantum-classical machine learning framework

Xiaodie Lin,[1] Zhenyu Chen,[1] and Zhaohui Wei[2,3,*]

[1]*Institute for Interdisciplinary Information Sciences, Tsinghua University, Beijing 100084, China*

[2]*Yau Mathematical Sciences Center, Tsinghua University, Beijing 100084, China*

[3]*Yanqi Lake Beijing Institute of Mathematical Sciences and Applications, Beijing 101407, China*

(Received 16 January 2023; accepted 26 May 2023; published 9 June 2023)

Quantifying entanglement for quantum states whose density matrices are unknown is a difficult task, but also becomes more and more necessary because of the fast development of quantum engineering. Machine learning provides practical solutions to this fundamental problem, where one has to train a proper machine learning model to predict entanglement measures of unknown quantum states based on experimentally measurable data, say, moments of density matrices or correlation data produced by local measurements. In this paper, we compare the performance of these two different machine learning approaches systematically. Particularly, we first show that the approach based on moments enjoys a remarkable advantage over that based on correlation data, though the cost of measuring moments is much higher. Next, since correlation data is much easier to obtain experimentally, we try to better its performance by proposing a hybrid quantum-classical machine learning framework for this problem, where the key is to train optimal local measurements, or even optimal tensor products of single-qubit observables, to generate more informative correlation data. Our numerical simulations show that the new hybrid framework brings us comparable performance with the approach based on moments to quantify entanglement, and furthermore, it turns out that the new hybrid framework has a nice noise-resistant capability when handling realistic correlation data.

DOI: 10.1103/PhysRevA.107.062409

I. INTRODUCTION

Quantum entanglement is a crucial resource for many quantum schemes and quantum protocols, such as quantum superdense coding [1], quantum teleportation [2], and quantum cryptography [3]. As a result, numerous measures have been raised to quantify the amount of entanglement contained in quantum states [4,5]. For bipartite pure states, entanglement measure is uniquely defined by the von Neumann entropy of subsystems. However, the landscape is far more complex for bipartite mixed states, where many important questions on entanglement quantifications have not been answered [6,7]. An even more complicated case is the quantifications of multipartite quantum entanglement, for which many different measures have been proposed but most of them are very hard to calculate [8–10]. It can be said that quantum entanglement has not been understood well theoretically.

Meanwhile, in recent years many subareas of quantum engineering have been under fast development, and because of this, detecting and even quantifying entanglement for quantum states whose density matrices are not known is becoming more and more realistic and necessary. However, the following two facts imply that this is a difficult task to fulfill. First, even if the underlying density matrix is given completely, determining whether a quantum state is entangled or not is already an NP-hard problem [11,12]. Second, when prior knowledge on target quantum states is missing, before looking into underlying entanglement we have to characterize these quantum states at least partially by performing quantum measurements. As a result, quantifying entanglement for unknown quantum states is an even harder problem than only certifying the existence of quantum entanglement for quantum states with known density matrices.

Existing methods that are able to quantify entanglement for unknown quantum states can be mainly divided into four branches. First, quantum tomography is the most popular approach adopted by quantum experimentalists when the size of target quantum states is small [13,14], where reconstructing quantum states allows us to look into the underlying entanglement. However, quantum tomography requires exponential cost, which is unbearable in high-dimensional quantum systems. Second, recently a new technique of quantifying entanglement, say, estimating the Rényi entropies, has been proposed, which performs random measurements on quantum states and then analyzes the outcome statistics [15–18]. Nevertheless, the cost of this technique is very high, where a large number of measurement settings are necessary. Third, device-independent protocols have been proposed to lower bound various entanglement measures [19–21]. These device-independent methods quantify entanglement exclusively from the observed measurement statistics on subsystems, thus independent of any assumptions on the interested quantum systems. In the realm of the noisy intermediate scale quantum (NISQ) era, device-independent protocols are attractive due to their efficiency and reliability. However, such device-independent protocols usually have limited applications in practice as they can provide nontrivial results only

*weizhaohui@gmail.com

when the observed quantum nonlocality is very strong. Fourth, in addition to these analytical methods, machine learning has also been utilized to provide practical solutions to quantify entanglement experimentally [22–25]. In such methods, different experimentally accessible data on quantum states is collected and fed into machine learning models such that the mappings from experimental data to target entanglement measures are learned, by which one can predict the entanglement measures of quantum states unseen before. In the current paper, we will focus on the fourth kind of method.

In fact, according to the sorts of involved experimental data, there exist already two different approaches to apply machine learning onto quantifying entanglement experimentally [22,23]. Specifically, in Ref. [22] the target entanglement measure is negativity, and for this the moment data of partially transposed states is fed into machine learning models as data features, which are usually very costly to obtain [26,27]. In Ref. [23], correlation data serves as data features to quantify entanglement, which is relatively convenient to prepare as one only needs to measure subsystems of target quantum states with a small set of local measurements chosen beforehand.

In this paper, we first show that several entanglement measures, like the relative entropy of entanglement, can also be quantified accurately using machine learning models based on the original moments of quantum state ρ defined as $\mu_m(\rho) = \mathrm{Tr}(\rho^m)$. Then we compare this new approach with the one in Ref. [23], and show that it can beat the latter easily in performance, though usually moment data are much harder to extract than correlation data. For example, a large number of measurement devices are already needed even if only $\mu_2(\rho)$ is measured [16,28].

Meanwhile, since correlation data comes from a small set of local measurements and is much easier to collect, it will be nice if we can somehow improve the performance of the machine learning approach based on correlation data. Note that in the above comparisons, correlation data is generated by a certain fixed set of local measurements for all training and test quantum states. Therefore, a possible way to improve the performance is to choose better local measurements for correlation data generations. For this, we propose a hybrid quantum-classical machine learning framework to quantify entanglement based on correlation data, where optimal local measurements, or even optimal tensor products of single-qubit observables, are trained to generate correlation data. Our numerical simulations show that the new framework allows the correlation method to achieve a comparable performance with the machine learning approach based on moments in entanglement quantification.

Lastly, we stress that the new hybrid framework has a nice noise-resistant capability, and enjoys decent performance when handling realistic correlation data produced by noisy quantum operations. Due to this, we expect that our new hybrid framework can be deployed on near-term quantum devices to quantify entanglement for unknown quantum states [29].

II. SETTINGS AND ENTANGLEMENT MEASURES

Consider a bipartite state ρ shared by two separated parties, Alice and Bob. Alice (Bob) has a set of measurement devices labeled by X (Y) to measure her (his) subsystem, and the possible measurement outcomes are labeled by A (B). After repeating the measurement many times, Alice and Bob calculate the joint conditional probabilities $p(ab|xy)$, which indicates the probability of obtaining outcomes $(a, b) \in A \times B$ upon selecting measurement settings $(x, y) \in X \times Y$. Suppose $\{M_x^a\}$ is the operator for the quantum measurement performed by Alice's measurement device $x \in X$, where $a \in A$, and analogously for $\{N_y^b\}$, then it holds that

$$p(ab|xy) = \mathrm{Tr}\big[\big(M_x^a \otimes N_y^b\big)\rho\big]. \tag{1}$$

A *correlation* $p = [p(ab|xy)]$ is a vector containing all the joint conditional probabilities of form $p(ab|xy)$.

We now turn to *moments* of quantum states, which are defined as [30,31]

$$\mu_m(\rho) = \mathrm{Tr}(\rho^m). \tag{2}$$

Clearly, $\mu_1(\rho) = \mathrm{Tr}(\rho) = 1$ and $\mu_2(\rho)$ is the *purity* of ρ. Experimentally, $\mu_m(\rho)$ can be measured directly by performing joint measurements on m copies of the same state ρ [30], while this operation is very hard with current quantum technologies, especially when m is large. To overcome this difficulty, techniques that can estimate $\mu_m(\rho)$ on single-copy states have also been developed [15].

A complete supervised machine learning system contains three ingredients: data features, data labels, and a machine learning model [32,33]. The training data features with correct labels are fed into the machine learning model, where the parameters contained in the learning model are trained properly such that the resulting system can predict labels of unknown test data precisely. In our problem, correlation data or moments serve as data features of quantum states, data labels are the values of target entanglement measures, and the machine learning model is supposed to learn an unknown nonlinear relationship between data features and data labels. According to the no free lunch theorem [34], a small target error rate implies that we need a large set of representative training data. However, it is well known that for bipartite mixed quantum states and multipartite quantum states, most entanglement measures are extremely hard to calculate, which means that it is hard for us to prepare correct labels for training data sets. According to the computation hardness and the importance of entanglement measures, in this paper we choose the coherent information and the relative entropy of entanglement as our target measures to quantify entanglement.

Coherent information is a fundamental quantity that measures the capability of transition of quantum information [35,36]. For an arbitrary bipartite quantum state $\rho \in \mathcal{H}_A \otimes \mathcal{H}_B$, its coherent information is defined as

$$I_C(\rho) = S(\rho_A) - S(\rho), \tag{3}$$

where $S(\rho)$ is the von Neumann entropy of ρ and $\rho_A = \mathrm{Tr}_B(\rho)$ is the subsystem in $\mathcal{H}_A$. A crucial property of the coherent information is that for any bipartite ρ, it holds that [37]

$$E_F(\rho) \geqslant E_D(\rho) \geqslant I_C(\rho), \tag{4}$$

where $E_F(\rho)$ and $E_D(\rho)$ are the two most important measures of entanglement, the entanglement of formation and the entanglement of distillation, respectively [38]. Therefore,

a good estimation of $I_C(\rho)$ implies that we obtain a very nontrivial piece of information on the amount of entanglement for ρ. Furthermore, it is not hard to see that the coherent information is very easy to calculate, which means that if we pick it as the data label, we can generate a large amount of training or test data at low cost.

Another quantity we will utilize is the relative entropy of entanglement [39], defined as

$$E_R(\rho) = \min_{\sigma\in\mathrm{SEP}} S(\rho\|\sigma) = \min_{\sigma\in\mathrm{SEP}} \mathrm{Tr}(\rho\log_2\rho - \rho\log_2\sigma), \quad (5)$$

where SEP denotes the set of all separable states. Relative entropy of entanglement has a good geometric interpretation, as $E_R(\rho)$ measures a certain "distance" between ρ and the set of separable states. Based on a machine learning model called *active learning*, we can numerically compute the relative entropy of entanglement for some particular quantum states with high accuracy [40]. At the same time, it turns out that the relative entropy of entanglement satisfies that [10]

$$E_F(\rho) \geqslant E_R(\rho) \geqslant E_D(\rho). \quad (6)$$

Therefore, similar to $I_C(\rho)$, estimating $E_R(\rho)$ of a quantum state ρ also helps us to obtain nontrivial information of $E_F(\rho)$ and $E_D(\rho)$.

III. COMPARISONS BETWEEN MACHINE LEARNING MODELS BASED ON CORRELATION DATA AND MOMENTS

In this section, we first present machine learning models that take correlation data and moments as data features, respectively, then we compare their performance in predicting both the coherent information and the relative entropy of entanglement systematically. For convenience, we call the former the correlation method and the latter the moment method.

A. Quantifying the coherent information

We begin with quantifying the coherent information of arbitrary three-dimensional bipartite quantum states $\rho \in \mathcal{H}^3 \otimes \mathcal{H}^3$. To generate more representative training data, we try to evenly sample quantum states according to the distribution of their coherent information. More concretely, we generate a random quantum state in $\mathcal{H}^d \otimes \mathcal{H}^d$ based on its spectral decomposition

$$\rho = \sum_{i=0}^{k-1} \lambda_i |u_i\rangle\langle u_i|, \quad (7)$$

where $k \in \{1, 2, \ldots, d^2\}$ is uniformly randomly chosen, the positive λ_i's are drawn uniformly from the interval [0,1) and normalized to satisfy $\sum_{i=0}^{k-1}\lambda_i = 1$, and $\{|u_i\rangle\}$ are the first k columns of a Haar random unitary U, i.e., $|u_i\rangle$ is the ith column of U. Here, we have $d = 3$. After sampling a random quantum state, we check its value of coherent information and decide whether to pick it or not, and thus ensure that the coherent information of the sampled quantum states distributes roughly evenly. However, due to the low efficiency of sampling quantum states with coherent information less than -1.5, in fact we only sample quantum states with coherent information ranging from -1.5 to $\log_2 3$. Specifically, we divide this range into 31 intervals of size 0.1, and in each of these intervals we sample 1291 quantum states randomly. Eventually, totally 40 021 states are randomly sampled to compose the set of quantum states for training.

To investigate the representativeness of the training quantum states, we calculate the average fidelity among them and obtain the value to be 0.2180, which means that these sampled quantum states distribute relatively far from each other on average. Therefore, our sampling method is reasonable, and gives us a representative set of training quantum states.

After sampling the training quantum states, we generate the corresponding training data features for the correlation method, which is achieved by performing the local measurements that maximize the violation of the Collins-Gisin-Linden-Masser-Popescu (CGLMP) inequality on the training quantum states [41,42], and then record the outcome statistics. More concretely, Alice's measurement A_k can be characterized by the eigenvectors

$$|r\rangle_{A_k} = \frac{1}{\sqrt{d}}\sum_{q=0}^{d-1}\exp\left(\frac{2\pi i}{d}q(r-\alpha_k)\right)|q\rangle_A, \quad (8)$$

and Bob's measurement B_l can be characterized by the eigenvectors

$$|r\rangle_{B_l} = \frac{1}{\sqrt{d}}\sum_{q=0}^{d-1}\exp\left(-\frac{2\pi i}{d}q(r-\beta_l)\right)|q\rangle_B, \quad (9)$$

where $0 \leqslant r \leqslant d-1$, $1 \leqslant k, l \leqslant N$, $\alpha_k = (k-1/2)/N$, $\beta_l = l/N$, and $N = |X| = |Y|$ [43]. In the current task, we let $d = 3$ and $N = 2$. That is, both Alice and Bob have two different measurement devices.

Meanwhile, to apply the moment method, we generate two different sets of training data, which contain different orders of moments. Specifically, for each quantum state ρ, one set contains $\{\mu_2(\rho_A), \mu_2(\rho)\}$ as its features, and the other contains $\{\mu_2(\rho_A), \mu_2(\rho), \mu_3(\rho_A), \mu_3(\rho)\}$ as its feature, where ρ_A is Alice's reduced density matrix.

To test the performance of the above three cases (one for the correlation method and two for the moment method), again we roughly evenly sample around 2000 quantum states according to the distribution of their coherent information, and then produce the corresponding test correlation data or moments of these states.

During the training stage, each training data set is fed into a four-hidden-layer fully connected neural network (FNN) with 400, 200, 100, and 50 neurons in each layer, respectively. After training, we test its performance with the corresponding test set sampled above. The results of all three cases are shown in Fig. 1. As we can see, the moment method that utilizes only the second order of moment already beats the correlation method in this task, whose corresponding mean squared errors (MSEs) are 0.0582 and 0.0035, respectively. In some sense this is not surprising since the number of measurement devices required by the moment method is much larger than that of the correlation method, and thus the moment data is more informative.

In addition, if we strengthen the moment method by also factoring in the third order of moment, apparent further improvements can be observed, where the MSE decreases to

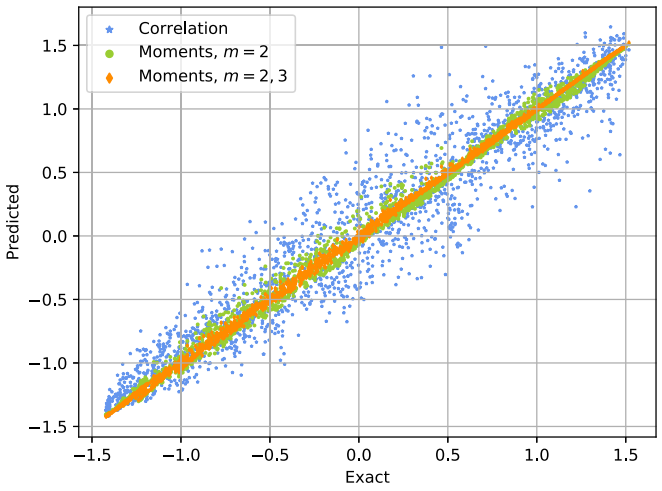

FIG. 1. The neural network predictions for $I_C(\rho)$. The blue stars represent the prediction values of the correlation method and the corresponding MSE is 0.0582. The green dots and orange diamonds represent the prediction values of the moment method with $m = 2$ and $m = 2, 3$, whose MSEs are 0.0035 and 0.0004, respectively.

0.0004, representing an excellent performance. As a result, compared with the correlation method, the moment method enjoys higher accuracy in coherent information quantification tasks.

We now increase the dimension of target quantum states $\rho \in \mathcal{H}^d \otimes \mathcal{H}^d$ to $d = 5, 8, 10$, and still aim to quantify the coherent information. In this case, the quantum state sampling procedure is similar to the three-dimensional case. Firstly, around 40 000 training quantum states are sampled roughly evenly by Eq. (7) according to the distribution of coherent information, and then around 2000 test quantum states are sampled similarly. The generations of data features for these quantum states are exactly the same as the previous task.

The training models for the moment method remain unchanged, i.e., a four-hidden-layer FNN with 400, 200, 100, and 50 neurons in each hidden layer is adopted. However, for the correlation method, since convolutional neural networks (CNNs, see Refs. [44,45] for further introductions) behave better than FNNs when dimension increases, in the current task we utilize CNNs to predict the coherent information instead of FNNs. Table I describes the structure and configuration details of our CNN model.

TABLE II. The MSEs of predicting the coherent information of random quantum states for different methods and dimensions.

Dimension	$d = 3$	$d = 5$	$d = 8$	$d = 10$
Correlation, $N = 2$	0.0582	0.0362	0.0212	0.0146
Moments, $m = 2$	0.0035	0.0034	0.0025	0.0026
Moments, $m = 2, 3$	0.0004	0.0010	0.0011	0.0010

Apply the trained models on the test data sets we have chosen, and the results for each case are listed in Table II.

Similar to the three-dimensional case, there still exists an obvious gap between the performance of the correlation method and that of the moment method. Furthermore, it is interesting to see that the improvements of introducing the third order of moment ($m = 2, 3$) over only using the second order ($m = 2$) decrease as the quantum dimension goes up. Therefore, considering the experimental difficulty of measuring moments, it is a good choice to set $m = 2$ when predicting coherent information for high-dimensional random quantum states.

Lastly, we would like to point out that both of the above approaches can be used to quantify entanglement for ground states of many-body quantum systems. For this purpose, we train the neural network models using pure quantum states in $\mathcal{H}^d \otimes \mathcal{H}^d$ with the form

$$|\psi\rangle \propto \alpha|\psi'\rangle + (1-\alpha)|\psi^{\text{sep}}\rangle, \tag{10}$$

where $\alpha \in [0, 1]$, $|\psi'\rangle$ is a random pure state generated by setting $k = 1$ in Eq. (7), and $|\psi^{\text{sep}}\rangle$ is a tensor product of two random pure states in $\mathcal{H}^d$. Here, we let $d = 8$. To generate the set of training quantum states, we first sample around 40 000 pure states according to Eq. (10) in such a way that their coherent information distributes roughly evenly, and then generate the data features similarly as before. An only difference is that, since $\mu_m(\rho) = 1$ for all pure states, we choose data features $\{\mu_2(\rho_A), \mu_3(\rho_A), \mu_4(\rho_A)\}$ for the moment method.

When choosing the structure for the neural network, it remains the same as before for the correlation method, while for the moment method we choose a two-hidden-layer FNN with 64 and 32 neurons in each hidden layer.

After training the neural networks, we test the performance of the two approaches with the Heisenberg XY model, which is a physical model consisting of two spins coupled via the Heisenberg XY interaction. For this model, the Hamiltonian

TABLE I. The structure and configuration details of the convolutional neural network. For each "·/·", the former parameter represents for $d = 5$ and the latter parameter represents for $d = 8, 10$.

Layers	Type	Neurons	Filters	Kernel size	Strides	Pool size
0–1	Convolution 2D	(None, 9/18, 9/18, 32)	32	$2 \times 2/3 \times 3$	1×1	–
1–2	Max-pooling 2D	(None, 8/16, 8/16, 32)	–	–	1×1	$2 \times 2/3 \times 3$
2–3	Convolution 2D	(None, 7/14, 7/14, 64)	64	$2 \times 2/3 \times 3$	1×1	–
3–4	Max-pooling 2D	(None, 6/12, 6/12, 64)	–	–	1×1	$2 \times 2/3 \times 3$
4–5	Convolution 2D	(None, 5/10, 5/10, 64)	64	$2 \times 2/3 \times 3$	1×1	–
5–6	Fully connected	(None, 64)	–	–	–	–
6–7	Fully connected	(None, 32)	–	–	–	–
7–8	Fully connected	(None, 1)	–	–	–	–

TABLE III. The MSEs of predicting the coherent information of ground states for different methods.

	XX model	XY model
Correlation, $N = 2$	0.0174	0.0284
Moments, $m = 4$	0.0122	0.0118

with periodic boundary conditions is given by [46,47]

$$H_{\mathrm{XY}} = -\frac{J}{2}\sum_{i=1}^{n}\left[(1+\gamma)\sigma_i^x\sigma_{i+1}^x + (1-\gamma)\sigma_i^y\sigma_{i+1}^y\right] - \frac{h}{2}\sum_{i=1}^{n}(-1)^{t\cdot i}\sigma_i^z, \tag{11}$$

where n is the number of sites, $\sigma_i^{x,y,z}$ denote the Pauli matrices at site $i \in \{1, 2, \ldots, n\}$, J specifies the coupling constant along two spins, $t \in \{0, 1\}$, and h is a magnetic field strength. Notice that the Heisenberg XX model ($\gamma = 0$) is a special case of this Hamiltonian. Here, we set $n = 6$, and consider the partition between the first three spins and the other three spins.

To obtain convincing test performance, we sample many different instances of the XY model and the XX model according to Eq. (11) and then use both the correlation method and the moment method to quantify the coherent information of their ground states. Specifically, for the XX model, we let $J = 2$, $t = 1$, and choose $h \in [0, 4]$ at intervals of size 0.01. For the XY model, we let $t = 0$, and then randomly sample $\gamma \in [-1, 0) \cup (0, 1]$, $J \in [0, 2]$, and $h \in [0, 4]$ to generate 2000 Hamiltonians such that the coherent information of their ground states distributes roughly evenly.

The overall prediction qualities of the correlation method and the moment method on these Hamiltonians are listed in Table III, where it can be seen that both methods exhibit very good performance, implying that our models can also perform well on real-world tasks.

B. Quantifying the relative entropy of entanglement

In addition to coherent information, we now show that the relative entropy of entanglement can also be predicted by the correlation method and the moment method. Recall that the relative entropy of entanglement is defined as an optimization problem over the set of separable states. Despite being convex, the set of separable states is still very hard to fully characterize, making the calculation of the relative entropy of entanglement NP-hard [48–50].

In Ref. [40], a technique to upper bound the relative entropy of entanglement was proposed based on active learning. Even though this method only provides upper bounds, Ref. [40] demonstrated that these upper bounds are quite tight for many quantum states, such as Werner states, isotropic states, and random bipartite quantum states with low dimensions. However, it should be stressed that the method introduced in Ref. [40] requires full descriptions of quantum states, i.e., the density matrix of the state, while our mission is quantifying entanglement based on experimentally measured quantities. In our task, we only utilize the active learning method to provide labels for our data sets, due to its high accuracy.

As usual, to generate representative training data, we would like to sample quantum states with evenly distributed relative entropy of entanglement. However, when the target values of relative entropy of entanglement are high, the sampling efficiency is very low. In addition, to provide high-precision labels for sampling quantum states, we have to calculate their relative entropy of entanglement using the active learning method introduced above, which is very costly. Both of these facts make it challenging for us to generate proper training and test data.

To prepare training data, here we focus on quantum states with the form

$$\rho = (1-\epsilon)\rho_0 + \epsilon|\psi_+\rangle\langle\psi_+|, \tag{12}$$

where $\epsilon \in [0, 1]$, ρ_0 is a random quantum state in $\mathcal{H}^d \otimes \mathcal{H}^d$ generated according to Eq. (7), and $|\psi_+\rangle = \frac{1}{\sqrt{d}}\sum_{i=1}^{d}|ii\rangle$. For each case of the dimension $d = 2, 3, 4$, 3 000 states are sampled by randomly selecting ϵ and ρ_0. Together with 1000 random separable states, totally 4000 states are sampled to serve as the training quantum states.

We next generate training data based on the sampled quantum states. For the correlation method, we prepare the training data by measuring the quantum states via the local measurements given in Eqs. (8) and (9), where for each party the number of measurement devices N is fixed as 2. For the moment method, the moments $\{\mu_m(\rho_A), \mu_m(\rho_B), \mu_m(\rho)\}$ are chosen as data features. Again, two sets of training data with $m = 2$ and $m = 2, 3$ are generated, in order to compare the power of moments of different orders.

As mentioned, the labels of the training data are provided by the active learning method. Meanwhile, the machine learning models for all three cases are the same, which is a four-hidden-layer FNN with 400, 200, 100, and 50 neurons in each layer.

After training, to estimate the performance of these models, we first run them on isotropic states, whose parametrized form is given by

$$\rho_{d_\epsilon}^{me} = \frac{(1-\epsilon)}{d^2}I_{d^2} + \epsilon|\psi_+\rangle\langle\psi_+|, \tag{13}$$

where $\epsilon \in [0, 1]$. Given an isotropic state, its relative entropy of entanglement can be analytically calculated [51], thus allowing us to benchmark the performance of models. We make the comparisons between the results given by all three cases and the exact results for $d = 2, 3, 4$. The results are depicted in Fig. 2, and the corresponding MSEs are shown in the first part of Table IV.

As illustrated, all three cases (one for the correlation method and two for the moment method) predict the relative entropy of entanglement of isotropic states correctly with high precision. Particularly, the results given by the active learning method, whose MSEs are in the order of $10^{-7}\sim10^{-5}$, match the analytical results given by Ref. [51] accurately.

Since the active learning method provides us a reliable way to calculate the relative entropy of entanglement, we now apply it to provide labels for random quantum states, which allows us to test our models on more general quantum

TABLE IV. The MSEs of predicting the relative entropy of entanglement for different methods and dimensions.

Dimension		$d = 2$	$d = 3$	$d = 4$
Isotropic	Correlation, $N = 2$	1.71×10^{-4}	4.14×10^{-4}	6.45×10^{-4}
	Moments, $m = 2$	3.57×10^{-5}	2.57×10^{-3}	9.08×10^{-4}
	Moments, $m = 2, 3$	4.88×10^{-5}	6.92×10^{-5}	1.37×10^{-4}
General	Correlation, $N = 2$	2.99×10^{-3}	6.90×10^{-3}	7.59×10^{-3}
	Moments, $m = 2$	2.26×10^{-4}	9.26×10^{-4}	1.45×10^{-3}
	Moments, $m = 2, 3$	2.01×10^{-4}	5.75×10^{-4}	9.12×10^{-4}

states, not just isotropic ones where the relative entropy of entanglement is analytically known.

Specifically, for each dimension, we sample 300 quantum states admitting the form Eq. (12), and combined with 100 random separable states, these 400 quantum states serve as test quantum states. The generations of data features for different methods are the same as before. Then we apply our trained FNNs to predict the relative entropy of entanglement of these quantum states, and the corresponding MSEs are listed in the second part of Table IV.

It can be seen that in this task the overall behaviors of the MSEs of the correlation method and the moment method are similar to those in the coherent information prediction tasks. Actually in this task the performance of the correlation method is even better, but a stable advantage of the moment method can still be observed.

IV. HYBRID QUANTUM-CLASSICAL FRAMEWORK ASSISTED CORRELATION METHOD

In Sec. III, we fixed local quantum measurements as the ones that achieve the maximal violation of the CGLMP inequality, and fixed the number of measurement devices for each party to be $N = 2$. Due to these two constraints, the power of the correlation method may be underestimated.

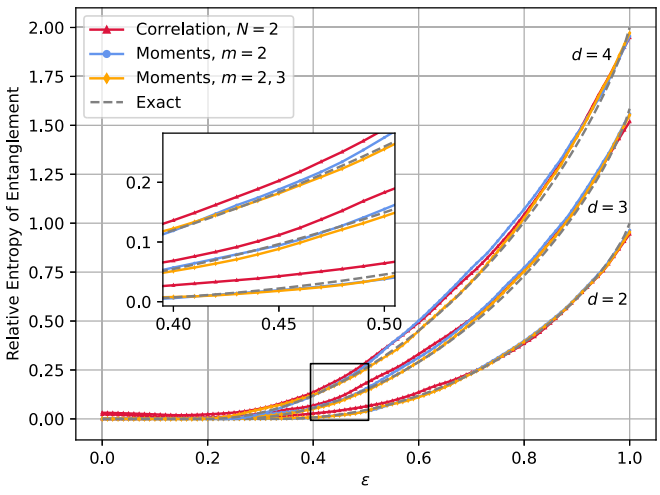

FIG. 2. The neural network predictions for $E_R(\rho^{me}_{d_\epsilon})$. The red triangles, blue dots, and orange diamonds represent the prediction values of the correlation method, the moment method with $m = 2$, and the moment method with $m = 2, 3$, respectively. The exact values are represented by the gray dashed line. All the corresponding MSEs are listed in the first part of Table IV.

Hence, a natural question is: Can we improve the performance of the correlation method by relaxing the constraints, say, enlarging the number of measurement devices N or changing the measurement devices?

A. More measurement devices

Intuitively, enlarging the set of available measurement devices can probably provide more information about target quantum states, and therefore may improve the performance of the correlation method. To check whether this idea works, we demonstrate it by setting $N = 3, 4$ in the coherent information prediction tasks for random quantum states.

For each quantum dimension $d = 3, 5, 8, 10$, the sampled training and test quantum states and the mathematical structures of machine learning models remain the same as before. The only difference is that now the training and test data sets are composed of measurement outcome statistics involving $N = 3, 4$ measurement devices, rather than 2. It turns out that very limited improvements are achieved by this change in predicting coherent information. Table V lists the corresponding MSEs.

The limited improvements given by increasing the number of measurement devices are unexpected, because more measurement devices should have revealed more information. A possible reason is that though the number of the measurement devices we have utilized is increased, they are still of the form in Eqs. (8) and (9). Therefore, to improve the performance of the correlation method further, we need to find out whether this form is optimal or not.

B. Learnable measurement devices

Looking back at all our previous machine learning models that have been discussed, we will see that all of them are classical models that deal with pure classical information, where all data features of involved quantum states are about correlation data or moments, which are essentially classical. However, we now need to choose better local measurements to generate more informative correlation data, which means that we have new quantum structures to learn. For this purpose,

TABLE V. The MSEs of predicting coherent information with fixed measurement devices.

Dimension	$d = 3$	$d = 5$	$d = 8$	$d = 10$
CGLMP, $N = 3$	0.0584	0.0356	0.0180	0.0170
CGLMP, $N = 4$	0.0540	0.0364	0.0183	0.0138

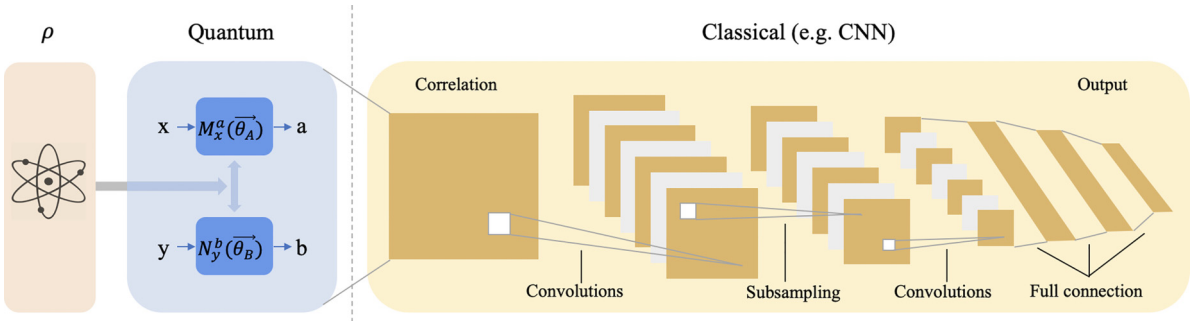

FIG. 3. The hybrid quantum-classical framework for the correlation method. (1) The input quantum state ρ, for which the full information is required. (2) The generation of correlation, where the local measurements M_x^a and N_y^b contain trainable variables. (3) The classical training part, which can be, for example, a CNN.

below we introduce a hybrid quantum-classical framework for our machine learning tasks.

In fact, a series of hybrid quantum-classical algorithms have been proposed [52–56], where the concept of parametrized quantum circuits (PQCs) is widely used to optimize a target function by iteratively tuning parameters contained in underlying quantum circuits. In our hybrid quantum-classical framework, the tuning target is quantum measurements. Since a general quantum measurement can be realized by first performing a unitary operation and then measuring in the computational basis, what we are aiming at is essentially learning $2N$ such unitary operators.

Our hybrid quantum-classical framework works as follows. First, since we want to find the best local measurements for our tasks, the entries of observables $\{M_x\}$ and $\{N_y\}$ are now regarded as trainable variables and will be updated repeatedly, which is the quantum part of our hybrid quantum-classical machine learning framework. Second, after choosing the training quantum states, we need to generate their training data features by measuring the parametrized observables $\{M_x\}$ and $\{N_y\}$, and then collecting the outcome statistics. Along with the correct labels, these data features will be fed into the classical learning part, which is the same as the previous models we have discussed. Figure 3 illustrates the whole framework. It is worth mentioning that according to our previous experience, different permutations of the measurement devices can result in quite a different prediction performance, especially when the training model is a CNN. Therefore, introducing trainable measurements will bring us the optimized permutation automatically.

We apply the hybrid quantum-classical machine learning framework to predict the coherent information of random quantum states for the cases $N = 2, 3, 4, 5$. The sampled training and test quantum states and the mathematical structure of the classical machine learning part remain the same as Sec. III A, where the dimension $d = 3, 5, 8, 10$. The results are listed in Fig. 4 and Table VI.

Comparing the case $N = 2$ with the old results in Table II, it can be seen that almost no improvement is achieved for each dimension except $d = 3$, which indicates that in generating statistics data the local measurements in Eqs. (8) and (9) are almost optimal for these cases. However, once we enlarge the number of possible measurement devices by only one, that is, $N = 3$, the situation becomes totally different, where the corresponding MSEs are 0.0206, 0.0121, and 0.0091 for dimensions 5, 8, and 10, respectively. Compared with the original version of the correlation method, 43.09%, 42.92%, and 37.67% improvements are achieved for dimensions 5, 8, and 10, respectively.

Furthermore, if we increase the number of measurement devices further, the improvements are even more remarkable. As illustrated in Fig. 4, when $d = 3$, our hybrid model with $N = 4$ has the same order of MSE as the moment method with $m = 2$, and when $d = 8, 10$, it is even comparable with that of the moment method with $m = 2, 3$. In fact, it turns out that even if we restrict Alice and Bob to perform the same set of local measurements, the obtained MSEs differ very little in high dimensions, e.g., $d = 5, 8, 10$. Therefore, a half number of the variables in the quantum part can be reduced to achieve a similar performance, hence facilitating the training efficiency.

Finally, in order to make the physical implementations more convenient, we restrict each local measurement performed by Alice and Bob to tensor products of single-qubit observables. Specifically, we regard a quantum state in $\mathcal{H}^d \otimes$

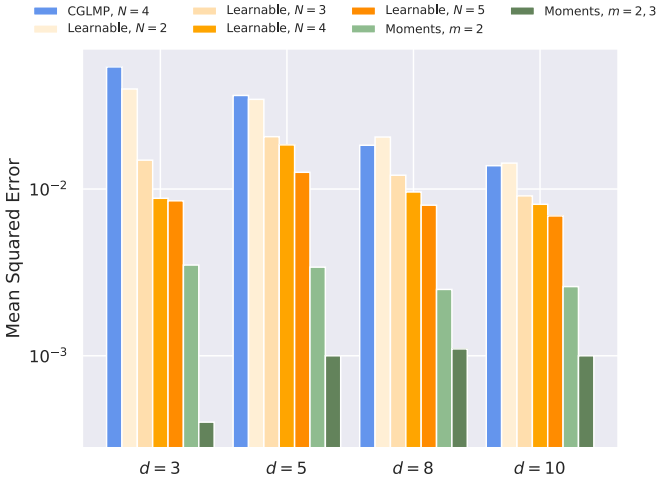

FIG. 4. Comparisons between the correlation method using the CGLMP measurements, learnable measurements, and the moment method. The MSEs of the correlation method using learnable measurements decrease as N increases. Particularly, when $N = 3$ an apparent improvement is achieved. When $N = 4$, the hybrid model even has the same order of MSE as the moment method with $m = 2, 3$ in high dimensions. The values of each MSE are listed in Table VI.

TABLE VI. The MSEs of predicting coherent information with learnable measurement devices.

Dimension	$d = 3$	$d = 5$	$d = 8$	$d = 10$
Learnable, $N = 2$	0.0398	0.0345	0.0205	0.0143
Learnable, $N = 3$	0.0149	0.0206	0.0121	0.0091
Learnable, $N = 4$	0.0088	0.0184	0.0096	0.0081
Learnable, $N = 5$	0.0085	0.0126	0.0080	0.0069

$\mathcal{H}^d$ as a $2n$-qubit state, where $n = \lceil \log_2 d \rceil$. The local observables performed by Alice and Bob admit the form $M_x = \bigotimes_{i=0}^{n-1} M_x^{(i)}$ and $N_y = \bigotimes_{i=0}^{n-1} N_y^{(i)}$, where $M_x^{(i)}$ and $N_y^{(i)}$ are observables on the ith qubit of Alice's and Bob's side, respectively. For convenience, we call such M_x and N_y qubit-based local measurements. Besides, to simplify the training procedure, Alice and Bob are assumed to perform the same set of qubit-based local measurements to produce the outcome statistics data. All experimental configurations are the same as before except for the form of the measured observables. The results are listed in Table VII.

It can be seen that compared with the previous setting, i.e., global measurements are allowed for each subsystem, the MSEs are slightly worse but comparable. Therefore, when replacing d-dimensional local measurements with qubit-based local observables, we can still quantify entanglement from the outcome statistics data with very good precision.

In addition, when $d = 3, 5, 10$, notice that $2^n > d$, that is, after the form of quantum measurements changes, the number of outcomes increases. As a result, when $N = 2, 3$, the performance of prediction is remarkably better than that of the previous results, which implies that the outcome statistics data brought by qubit-based local observables is more informative than before. However, when N increases to 4,5, the performance of prediction is a little bit worse. Nevertheless, in all cases our hybrid model with qubit-based local observables still has the same order of MSEs as the moment method.

Recall that though the moment method has very good performance, the experimental cost of measuring moments is much higher than that of generating correlation data. Therefore, our result clearly implies that our hybrid quantum-classical framework of machine learning largely overcomes this difficulty, and achieves similar performance.

C. Noise resistance of the hybrid framework

In practice, collecting ideal outcome statistics data is challenging due to imperfect measurement devices and shot noise [57–60]. Therefore, it is very important to estimate the impact

TABLE VII. The MSEs of predicting the coherent information with learnable qubit-based local measurement devices.

Dimension	$d = 3$	$d = 5$	$d = 8$	$d = 10$
Learnable, $N = 2$	0.0197	0.0272	0.0213	0.0108
Learnable, $N = 3$	0.0105	0.0190	0.0123	0.0091
Learnable, $N = 4$	0.0102	0.0155	0.0101	0.0090
Learnable, $N = 5$	0.0097	0.0162	0.0099	0.0079

TABLE VIII. The MSEs of predicting the coherent information of noisy test quantum states with models trained by noiseless training quantum states.

Dimension	$d = 3$	$d = 5$	$d = 8$	$d = 10$
Learnable, $N = 2$	0.0399	0.0371	0.0215	0.0149
Learnable, $N = 3$	0.0151	0.0234	0.0128	0.0101
Learnable, $N = 4$	0.0086	0.0216	0.0095	0.0079
Learnable, $N = 5$	0.0093	0.0138	0.0088	0.0074

of small errors in collecting outcome statistics data on the performance of our hybrid framework. It turns out that our models enjoy a nice noise-resistant capability. To demonstrate that this is indeed the case, for simplicity we now suppose that all test quantum states suffer from a depolarizing noise before they are measured, and apparently this will bring errors to the underlying outcome statistics data.

Specifically, let us go back to the previously trained hybrid quantum-classical models for predicting coherent information (see Table VI). We also use the same set of test quantum states $\rho \in \mathcal{H}^d \otimes \mathcal{H}^d$ sampled there, where $d = 3, 5, 8, 10$. However, before measuring these test quantum states via the same quantum measurements, we adjust them with the transformation

$$\rho_{\text{noisy}} = (1 - \epsilon)\rho + \frac{\epsilon}{d^2} I_{d^2}, \tag{14}$$

where I_{d^2}/d^2 is the maximally mixed state. Here we let $\epsilon = 0.01$. Without further training, we apply the same model with learnable measurements previously trained in Sec. IV B to predict the coherent information of these test quantum states based on the imperfect outcome statistics data, and the results are listed in Table VIII.

Compared with the results in Table VI, it can be seen that the performance of the predictions on noisy quantum states is comparable to that on noiseless quantum states, and the average increment of MSE is only 9.37×10^{-4}. Therefore, our hybrid framework enjoys a nice noise-resistant capability, and errors in outcome statistics data produced in practical physical implementations do not hurt the performance of our models much.

V. CONCLUSION

Quantifying entanglement experimentally is a very challenging task today. However, considering the profound importance of quantum entanglement and the fast developments of quantum industries, fulfilling this kind of tasks will probably become a daily routine in the future. As a result, finding realistic and economical solutions for this problem from the viewpoint of engineering is extremely necessary, and a promising approach for this is using machine learning methods, which in recent years have been widely applied in quantum information processing tasks [61–66].

In this paper, we focus on two known machine learning approaches for quantifying entanglement experimentally, one using moments as data features and the other using correlation data. We systematically compare their performance in

predicting the coherent information and the relative entropy of entanglement. According to our results, the moment method behaves much better than the correlation method, which is consistent with the intuition. In fact, as mentioned, each moment is a quantity related to the eigenvalues of the corresponding density matrix, and all the moments together in principle can pin down the essential information of the density matrix. Hence, the moment method naturally enjoys a remarkable advantage in quantifying entanglement. However, estimating moments is much harder than correlation data.

This motivates us to improve the performance of the correlation method in quantifying entanglement. For this, we propose a hybrid quantum-classical framework of machine learning models to generate more informative correlation data. Specifically, we studied two possible directions to achieve this, where one directly enlarges the number of local measurements fixed beforehand to produce more informative correlation data, and the other adds a new quantum module for the machine learning model to search for better local measurements or even tensor products of qubit observables utilized in correlation data generations, and at the same time increases their number. It turns out that the former direction only has a little improvement, while the latter is much better, and it even achieves comparable performance with the moment method.

Furthermore, we have shown that our models exhibit a nice noise-resistant capability, and still enjoy decent performance when handling realistic correlation data produced by noisy quantum operations. Therefore, our hybrid framework is expected to have potential applications in quantifying entanglement for unknown quantum states on near-term quantum devices.

ACKNOWLEDGMENTS

This work was supported by the National Key R&D Program of China, Grants No. 2018YFA0306703 and No. 2021YFE0113100, and the National Natural Science Foundation of China, Grants No. 61832015 and No. 62272259.

[1] C. H. Bennett and S. J. Wiesner, Phys. Rev. Lett. **69**, 2881 (1992).
[2] C. H. Bennett, G. Brassard, C. Crépeau, R. Jozsa, A. Peres, and W. K. Wootters, Phys. Rev. Lett. **70**, 1895 (1993).
[3] A. K. Ekert, Phys. Rev. Lett. **67**, 661 (1991).
[4] R. Horodecki, P. Horodecki, M. Horodecki, and K. Horodecki, Rev. Mod. Phys. **81**, 865 (2009).
[5] L. Amico, R. Fazio, A. Osterloh, and V. Vedral, Rev. Mod. Phys. **80**, 517 (2008).
[6] M. Horodecki, P. Horodecki, and R. Horodecki, Phys. Rev. Lett. **80**, 5239 (1998).
[7] V. Vedral, M. B. Plenio, M. A. Rippin, and P. L. Knight, Phys. Rev. Lett. **78**, 2275 (1997).
[8] A. R. R. Carvalho, F. Mintert, and A. Buchleitner, Phys. Rev. Lett. **93**, 230501 (2004).
[9] H. Barnum and N. Linden, J. Phys. A: Math. Gen. **34**, 6787 (2001).
[10] V. Vedral and M. B. Plenio, Phys. Rev. A **57**, 1619 (1998).
[11] L. Gurvits, J. Comput. Syst. Sci. **69**, 448 (2004).
[12] S. Gharibian, Quantum Inf. and Comput. **10**, 343 (2010).
[13] I. L. Chuang and M. A. Nielsen, J. Mod. Opt. **44**, 2455 (1997).
[14] J. F. Poyatos, J. I. Cirac, and P. Zoller, Phys. Rev. Lett. **78**, 390 (1997).
[15] S. J. van Enk and C. W. J. Beenakker, Phys. Rev. Lett. **108**, 110503 (2012).
[16] T. Brydges, A. Elben, P. Jurcevic, B. Vermersch, C. Maier, B. P. Lanyon, P. Zoller, R. Blatt, and C. F. Roos, Science **364**, 260 (2019).
[17] H.-Y. Huang, R. Kueng, and J. Preskill, Nat. Phys. **16**, 1050 (2020).
[18] O. Sotnikov, I. Iakovlev, A. Iliasov, M. Katsnelson, A. Bagrov, and V. Mazurenko, npj Quantum Inf. **8**, 41 (2022).
[19] T. Moroder, J.-D. Bancal, Y.-C. Liang, M. Hofmann, and O. Gühne, Phys. Rev. Lett. **111**, 030501 (2013).
[20] Z. Wei and L. Lin, Phys. Rev. A **103**, 032215 (2021).
[21] L. Lin and Z. Wei, Phys. Rev. A **104**, 062433 (2021).
[22] J. Gray, L. Banchi, A. Bayat, and S. Bose, Phys. Rev. Lett. **121**, 150503 (2018).
[23] X. Lin, Z. Chen, and Z. Wei, arXiv:2104.12527.
[24] J. Roik, K. Bartkiewicz, A. Černoch, and K. Lemr, Phys. Lett. A **446**, 128270 (2022).
[25] J. Y. Khoo and M. Heyl, Phys. Rev. Res. **3**, 033135 (2021).
[26] Y. Zhou, P. Zeng, and Z. Liu, Phys. Rev. Lett. **125**, 200502 (2020).
[27] A. Elben, R. Kueng, H. Y. R. Huang, R. van Bijnen, C. Kokail, M. Dalmonte, P. Calabrese, B. Kraus, J. Preskill, P. Zoller, and B. Vermersch, Phys. Rev. Lett. **125**, 200501 (2020).
[28] B. Vermersch, A. Elben, M. Dalmonte, J. I. Cirac, and P. Zoller, Phys. Rev. A **97**, 023604 (2018).
[29] J. Preskill, Quantum **2**, 79 (2018).
[30] A. K. Ekert, C. M. Alves, D. K. L. Oi, M. Horodecki, P. Horodecki, and L. C. Kwek, Phys. Rev. Lett. **88**, 217901 (2002).
[31] P. Horodecki, Phys. Rev. Lett. **90**, 167901 (2003).
[32] M. Mohri, A. Rostamizadeh, and A. Talwalkar, *Foundations of Machine Learning* (MIT Press, Cambridge, 2018).
[33] S. Shalev-Shwartz and S. Ben-David, *Understanding Machine Learning: From Theory to Algorithms* (Cambridge University Press, Cambridge, 2014).
[34] D. H. Wolpert and W. G. Macready, IEEE Trans Evol. Comput. **1**, 67 (1997).
[35] B. Schumacher and M. A. Nielsen, Phys. Rev. A **54**, 2629 (1996).
[36] S. Lloyd, Phys. Rev. A **55**, 1613 (1997).
[37] M. F. Cornelio, M. C. de Oliveira, and F. F. Fanchini, Phys. Rev. Lett. **107**, 020502 (2011).
[38] C. H. Bennett, D. P. DiVincenzo, J. A. Smolin, and W. K. Wootters, Phys. Rev. A **54**, 3824 (1996).
[39] V. Vedral, Rev. Mod. Phys. **74**, 197 (2002).
[40] S.-Y. Hou, C. Cao, D. Zhou, and B. Zeng, Quantum Sci. Technol. **5**, 045019 (2020).
[41] D. Collins, N. Gisin, N. Linden, S. Massar, and S. Popescu, Phys. Rev. Lett. **88**, 040404 (2002).

[42] S. Zohren and R. D. Gill, Phys. Rev. Lett. **100**, 120406 (2008).
[43] J. Barrett, A. Kent, and S. Pironio, Phys. Rev. Lett. **97**, 170409 (2006).
[44] Y. Lecun, L. Bottou, Y. Bengio, and P. Haffner, Proc. IEEE **86**, 2278 (1998).
[45] S. Albawi, T. A. Mohammed, and S. Al-Zawi, in *2017 Proceedings of the International Conference on Engineering and Technology (ICET)* (IEEE, New York, 2017), pp. 1–6.
[46] Y.-X. Xie and Y.-Y. Gao, Laser Phys. Lett. **16**, 045202 (2019).
[47] Z. N. Ha, *Quantum Many-Body Systems in One Dimension* (World Scientific, Singapore, 1996), Vol. 12.
[48] Y. Huang, New J. Phys. **16**, 033027 (2014).
[49] S. Lu, S. Huang, K. Li, J. Li, J. Chen, D. Lu, Z. Ji, Y. Shen, D. Zhou, and B. Zeng, Phys. Rev. A **98**, 012315 (2018).
[50] A. C. Doherty, P. A. Parrilo, and F. M. Spedalieri, Phys. Rev. Lett. **88**, 187904 (2002).
[51] T.-C. Wei, Phys. Rev. A **78**, 012327 (2008).
[52] A. Peruzzo, J. McClean, P. Shadbolt, M.-H. Yung, X.-Q. Zhou, P. J. Love, A. Aspuru-Guzik, and J. L. O'brien, Nat. Commun. **5**, 4213 (2014).
[53] K. Mitarai, M. Negoro, M. Kitagawa, and K. Fujii, Phys. Rev. A **98**, 032309 (2018).
[54] J. R. McClean, J. Romero, R. Babbush, and A. Aspuru-Guzik, New J. Phys. **18**, 023023 (2016).
[55] A. Mari, T. R. Bromley, J. Izaac, M. Schuld, and N. Killoran, Quantum **4**, 340 (2020).
[56] J. Liu, K. H. Lim, K. L. Wood, W. Huang, C. Guo, and H.-L. Huang, Sci. China Phys. Mech. Astron. **64**, 290311 (2021).
[57] P. Krantz, M. Kjaergaard, F. Yan, T. P. Orlando, S. Gustavsson, and W. D. Oliver, Appl. Phys. Rev. **6**, 021318 (2019).
[58] W. Nagourney, J. Sandberg, and H. Dehmelt, Phys. Rev. Lett. **56**, 2797 (1986).
[59] J. Harris, R. W. Boyd, and J. S. Lundeen, Phys. Rev. Lett. **118**, 070802 (2017).
[60] D. F. V. James, P. G. Kwiat, W. J. Munro, and A. G. White, Phys. Rev. A **64**, 052312 (2001).
[61] K. Bharti, T. Haug, V. Vedral, and L.-C. Kwek, AVS Quantum Sci. **2**, 034101 (2020).
[62] V. Dunjko and H. J. Briegel, Rep. Prog. Phys. **81**, 074001 (2018).
[63] N. Asif, U. Khalid, A. Khan, T. Q. Duong, and H. Shin, Sci. Rep. **13**, 1562 (2023).
[64] Á. Sáiz, J.-E. García-Ramos, J. M. Arias, L. Lamata, and P. Pérez-Fernández, Phys. Rev. C **106**, 064322 (2022).
[65] J. Gao, L.-F. Qiao, Z.-Q. Jiao, Y.-C. Ma, C.-Q. Hu, R.-J. Ren, A.-L. Yang, H. Tang, M.-H. Yung, and X.-M. Jin, Phys. Rev. Lett. **120**, 240501 (2018).
[66] A. Valenti, E. van Nieuwenburg, S. Huber, and E. Greplova, Phys. Rev. Res. **1**, 033092 (2019).